Journal of Cardiology 66 (2015) 28–35

Contents lists available at ScienceDirect

Journal of Cardiology

journal homepage: www.elsevier.com/locate/jjcc

Original article

Interleukin-18-induced atherosclerosis involves CD36 and NF-κB crosstalk in Apo E−/− mice

Owais Mohammad Bhat (MSc)[a], P. Uday Kumar (MD)[b], N.V. Giridharan (PhD)[c], Deepak Kaul (PhD)[a], M.J. Mahesh Kumar (PhD)[d], Veena Dhawan (PhD)[a,*]

[a] Department of Experimental Medicine and Biotechnology, Postgraduate Institute of Medical Education and Research (PGIMER), Chandigarh, India
[b] National Centre for Laboratory Animal Sciences (NCLAS), Hyderabad, Department of Histopathology, National Institute of Nutrition (NIN), Hyderabad, India
[c] Amrita School of Nanosciences & Molecular Medicine, Amrita Institute of Medical Sciences, Amrita Viswavidyapeedham, Kochi, Kerala, India
[d] Animal House, Centre for Cellular and Molecular Biology (CCMB), Hyderabad, India

ARTICLE INFO

Article history:
Received 2 July 2014
Received in revised form 15 September 2014
Accepted 6 October 2014
Available online 1 December 2014

Keywords:
Recombinant interleukin-18
Atherosclerosis
CD36
Liver X receptor alpha
Nuclear factor kappa-B

ABSTRACT

Objective: Interleukin (IL)-18 is a pleotropic cytokine involved in various inflammatory disorders. The transcription factor, nuclear factor kappa-B (NF-κB), is thought to play an important role in IL-18 signaling. The present study proposes a novel role for IL-18 in cholesterol efflux and plaque stability and demonstrates that pyrrolidine dithiocarbamate (PDTC), a NF-κB inhibitor blocks IL-18 signaling in apolipoprotein (Apo) E−/− mice.

Methods: Three groups of normal chow-diet-fed, male Apo E−/− mice, aged 12 weeks (n = 6/group) were employed: Gp I, PBS (2 mo); Gp II, recombinant (r)IL-18 (1 mo) followed by PBS (1 mo); Gp III, rIL-18 (1 mo) followed by PDTC (1 mo).

Results: Significantly augmented expression of IL-18 receptor (R)α by fluorescence-activated cell sorting analysis and plasma IL-18 was observed in Gp II. There was a significant increase in total cholesterol and low-density lipoprotein cholesterol whereas high-density lipoprotein cholesterol was significantly decreased in Gp II. However, this pattern was reversed in Gp III. Significantly augmented mRNA expression of IL-18, CD36, matrix metalloproteinase (MMP)-9, and NF-κB was observed in Gp II but liver X receptor alpha (LXR-α) gene was significantly reduced. A significant increase in frequency of atherosclerotic lesions was observed in Gp II animals, whereas there was a significant decrease in the Gp III.

Conclusion: IL-18 administration initiates inflammatory cascade by binding with IL-18 Rα via NF-κB which is involved in progression and destabilization of atherosclerotic plaques in Apo E−/− mice. This study also reveals that NF-κB blockade with PDTC, blocks IL-18 signaling through down-regulation of IL-18, IL-18 Rα, CD36, and MMP-9, thus reducing inflammation and restoring plaque instability via upregulation of LXR-α.

Introduction

Endothelial dysfunction, imbalanced lipid metabolism, and a maladaptive inflammatory immune response are hallmarks of atherosclerotic disease. The nuclear receptors, i.e. liver X receptor alpha (LXR-α) and peroxisome proliferator-activated receptors (PPARs) are not only involved in cholesterol efflux via macrophages [1], but also regulate the expression of many genes involved in the production of proinflammatory cytokines, adhesion molecules, and scavenger receptors (CD36, SR-A, SR-B1) that control the native and oxidized low-density lipoprotein (ox-LDL) uptake, an important step in foam cell formation [2]. These oxidized lipids activate nuclear factor-κB (NF-κB) which transcriptionally regulates many cellular genes implicated in early immune, acute-phase, and inflammatory responses [3]. Acute or chronic activation of NF-κB, is also shown to activate matrix metalloproteinase-9 (MMP-9) resulting in atherosclerotic plaque instability and rupture [4]. Therefore, inhibition of NF-κB is functionally important and suggests therapies for diseases related to the acute or chronic activation of NF-κB.

The apolipoprotein E knockout (Apo E−/− mice) mouse fed on a standard chow diet, spontaneously develops atherosclerotic

* Corresponding author at: Department of Experimental Medicine and Biotechnology, Research Block-B, Postgraduate Institute of Medical Education and Research (PGIMER), Chandigarh 160012, India. Tel.: +91 172 2747585x5235; fax: +91 172 2744401.
E-mail address: veenad2001@yahoo.com (V. Dhawan).

http://dx.doi.org/10.1016/j.jjcc.2014.10.012
0914-5087/

lesions in the aorta and its major branches over a short period with a distribution similar to human atherosclerosis and can be accelerated by feeding a Western diet [5,6]. Therefore Apo E−/− mice were chosen as an animal model in our study.

Interleukin-18 (IL-18) is a proinflammatory cytokine with pleotropic properties [5] and induced IL-18 expression has been observed in unstable human atherosclerotic plaques from asymptomatic patients [7]. An over expression of murine IL-18 binding protein, the endogenous inhibitor of IL-18 is shown to reduce atherosclerotic lesion development in Apo E−/− mice [8]. IL-18 acts by binding to its receptor (IL-18 Rα), is expressed on a variety of cells, and initiates signaling [9].

In view of the above, we hypothesized that exogenous IL-18 treatment may aggravate atherosclerosis by modulating expression of crucial genes and that, PDTC a specific NF-κB inhibitor may inhibit IL-18-induced signaling and thereby halt atherosclerotic progression. Here, we report a novel pathway of IL-18-induced atherosclerosis involving CD36 and NF-κB crosstalk and demonstrate that pyrrolidine dithiocarbamate (PDTC) successfully inhibits IL-18-induced atherosclerosis.

Materials and methods

Lyophilized recombinant mouse IL-18 (rIL-18) was purchased from R&D Systems, Inc, Minneapolis, MN, USA (Catalog#: B002-5) and reconstituted as per manufacturer's protocol. PDTC (Catalog no P8765) was purchased from Sigma Aldrich, St. Louis, MO, USA.

IL-18 treatment

Eighteen male Apo E−/− mice (12 weeks old), with the C57BL/6 strain background, were obtained from the Centre for Cellular and Molecular Biology (CCMB), Hyderabad, India. The animal protocol was approved by the Institute Animal Ethics Committee (IAEC) (reference No. 49/IAEC/237) of PGIMER, Chandigarh. All the animal procedures were performed following the US National Institutes of Health protocol. Polymerase chain reaction (PCR) was used to identify mice homozygous for Apo E−/− [10]. After acclimatization, mice were divided into three groups of 6. Group I received daily intraperitoneal injections of phosphate buffered saline (PBS) (containing 0.1% bovine serum albumin and 1% sucrose), while Group II received daily intraperitoneal injections of rIL-18 (30 ng/g body weight) for one month followed by PBS for one month [11]. Group III received daily intraperitoneal injections of rIL-18 (30 ng/g body weight) for one month followed by PDTC for one month (10 mg/kg body weight) [12].

Processing of tissues

At the end of the experimental period, mice were euthanized by intraperitoneal injection of ketamine plus xylazine (90 + 10 mg/kg body weight) [11]. Terminal blood samples were collected by puncture of the right ventricle, and mice were perfused with PBS. Hearts were separated from the aorta at the base, embedded in optimum cutting temperature (OCT, cryo embedding media) and frozen at −80 °C. Aortic tissue was removed from the ascending aorta to the level of diaphragm, embedded in OCT and frozen at −80 °C for immunohistochemical analysis. Hearts were transversely cut into two parts. The half containing the apex was stored at −80 °C for molecular biology work. The other half comprising the base and origin of the aorta was embedded in OCT and multiple frozen sections were cut. The leftover frozen tissue remnant was then brought to room temperature and fixed in 10% buffered formalin for histopathological evaluation and Masson's trichrome staining [11].

Quantification of atherosclerotic lesions

Assessment and quantification of atherosclerotic lesions was carried out by two independent pathologists in a blinded manner. Size of the atherosclerotic lesions was determined in sections from ascending aorta (four), cut 8-μm thick, collected at 80-μm intervals, starting at the region where aortic sinus becomes the ascending aorta and lesion areas, defined by Oil Red O (ORO) staining of the intima, were determined using Image-Pro software (Image J; Media Cybernetics Inc, Rockville, MD, USA). Mean lesion area derived from the 4 serial sections was taken as the mean lesion size for each animal [13].

Immunohistochemistry

Briefly, frozen tissue sections (8 μm) of tissues were fixed with acetone for 20 min, followed by endogenous peroxidase blocking with 0.3% H_2O_2 solution in methanol. Sections were incubated with 2.5% horse serum followed by incubation with respective primary antibodies, overnight at 4 °C. Sections were subsequently incubated with biotinylated secondary antibodies and a streptavidin-peroxidase complex (PK-7800, Vector Laboratories, Burlingame, CA, USA), developed with diamino benzidine (DAB) substrate (0.05% DAB–0.015% H_2O_2 in PBS; Cat No. D 5637, Sigma Aldrich) and counterstained with hematoxylin. Slides were dehydrated and mounted with DPX. For immunostaining: anti-mouse liver X receptor-α (LXR-α) goat polyclonal antibody (sc-1201, 1:50 dilution; Santa Cruz Biotechnology, Dallas, TX, USA), anti-mouse CD36 rabbit polyclonal antibody (ab78054, 2.5 μg/ml; Abcam, Cambridge, MA, USA), anti-mouse nuclear factor-κB (NF-κB p65 antibody, RelA) rabbit polyclonal antibody [PC137, 1:100 dilution; Calbiochem (EMD Millipore, Billerica, MA, USA)] and anti-mouse MMP-9 goat polyclonal antibody (sc-6840, 1:50 dilution; Santa Cruz Biotechnology) were used respectively.

Serum cholesterol and lipoprotein profile

At the end of the study, serum total cholesterol (TC; Cat No. 11506), triglycerides (TG; Cat No. 11528), and high-density lipoprotein cholesterol (HDL-C; Cat No. 11648) levels were determined using commercially available enzymatic kits (Biosystems Kit, Barcelona, Spain). Low-density lipoprotein cholesterol (LDL-C) and very low-density lipoprotein-cholesterol (VLDL-C) concentrations were calculated using Friedwald's formula [14].

Friedwald's formula:

$$\text{LDL-C} = \text{TC} - \left(\text{HDL-C} + \frac{\text{TG}}{5}\right)$$

$$\text{VLDL-C} = \frac{\text{TG}}{5}$$

Therefore, LDL-C = TC − (HDL-C + VLDL-C). Hence, VLDL-C = TC − (HDL-C + LDL-C). So above equation is verified and is correct.

Fluorescence-activated cell sorting analysis of IL-18 Rα

IL-18 Rα expression was analyzed in the blood using allophycocyanin (APC)-conjugated rat monoclonal anti-mouse IL-18 Rα antibody (R&D, Minneapolis, MN, USA; Cat. No: FAB1216A, Lot No: ABKA02, 10 μg/ml). Tubes were incubated with fluorescence-activated cell sorting (FACS) lysis buffer for 10 min at RT and cells were washed twice in flow cytometry staining buffer. IL-18 Rα expression was analyzed using Becton Dickinson FACS Aria II flow cytometer using DIVA software (Becton Dickinson, Franklin Lakes, NJ, USA).

Real time-PCR studies

Due to limited availability of the tissues, the mRNA levels of LXR-α, CD36, NF-κB, and IL-18 were determined in the heart and MMP-9 was determined in the aorta by RT-PCR. The following mouse specific primers were used: LXR-α: F-5′-CCTTCCTCAAGGACTTCAGTTACAA-3′, R-5′-CATGGCTCTGGAGAACTCAAAGAT-3′; CD36: F-5′-ACATTTGCAGGTCTATCTACG-3′, R-5′-AATGGTTGTCTGGATTCTGG-3′; MMP-9: F-5′-CATTCGCGTGGATAAGGAGT-3′, R-5′-CACTGCAGGAGGTCGTAGG-3′; IL-18: F-5′-ACGTGTTCCAGGACACAACA-3′, R-5′-ACAAACCCTCCCCACCTAAC-3′; NF-κB: F-5′-TGGG GGCCTTGCTTGGCAAC-3′, R-5′-GAGGTCCCCAGGGGTGTGGG-3′; and β-Actin: F-5′-GCATTGCTGACAGGATGCAG-3′, R-5′-CCTGCT TGCTGATCCACATC-3′. Expression as fold increase/decrease was calculated using the $2^{-\Delta\Delta CT}$ method [15]. The data were expressed as relative mRNA expression normalized to mouse β-actin mRNA expression.

IL-18 enzyme-linked immunosorbent assay

IL-18 was determined in the plasma samples with commercially available mouse specific IL-18 enzyme-linked immunosorbent assay kit (7625; MBL, Nagoya, Japan). The sensitivity of the kit was 25 pg/ml. Results are expressed in units as pg/ml.

Statistical methods

All data are expressed as mean ± SD. Data analyses were performed using Graph Pad Prism 5.00.288 software (La Jolla, CA, USA). Statistical analysis between the groups was done by unpaired Student's '*t*' test and ANOVA after testing that the data complied with the constraints of parametric analysis. Where parametric analysis was not permissible, analysis between groups was conducted using the Tukey test. Values with $p \leq 0.05$ were considered statistically significant.

Results

IL-18 levels and IL-18 Rα expression in IL-18-treated Apo E−/− mice

Plasma IL-18 levels were found to be significantly increased in Group II animals vs. Group I (170 ± 9.16 pg/ml vs. 1178.66 ± 8.08 pg/ml, $p < 0.001$), whereas these levels were significantly decreased in Group III vs. II animals (1178.66 ± 8.08 pg/ml vs. 883.33 ± 76.37 pg/ml, $p < 0.001$) (Fig. 1A). IL-18 mRNA expression in the heart of Apo E−/− mice was also augmented by 6-fold in Group II mice as compared to the Group I animals ($p < 0.001$, Fig. 1B) and was found to be significantly reduced in Group III mice ($p < 0.001$, Fig. 1B). FACS analysis revealed that in Group II IL-18 Rα expression was significantly enhanced on peripheral blood mononuclear cells (15.2 ± 1.3 vs. 59.7 ± 3.05), whereas it was downregulated in Group III (59.7 ± 3.05 vs. 12.76 ± 2.83) ($p < 0.001$, Fig. 1C and D).

Lipids and lipoproteins in IL-18-treated Apo E−/− mice

When compared with Group I, there was non-significant change in the body weight of Group II and Group III mice

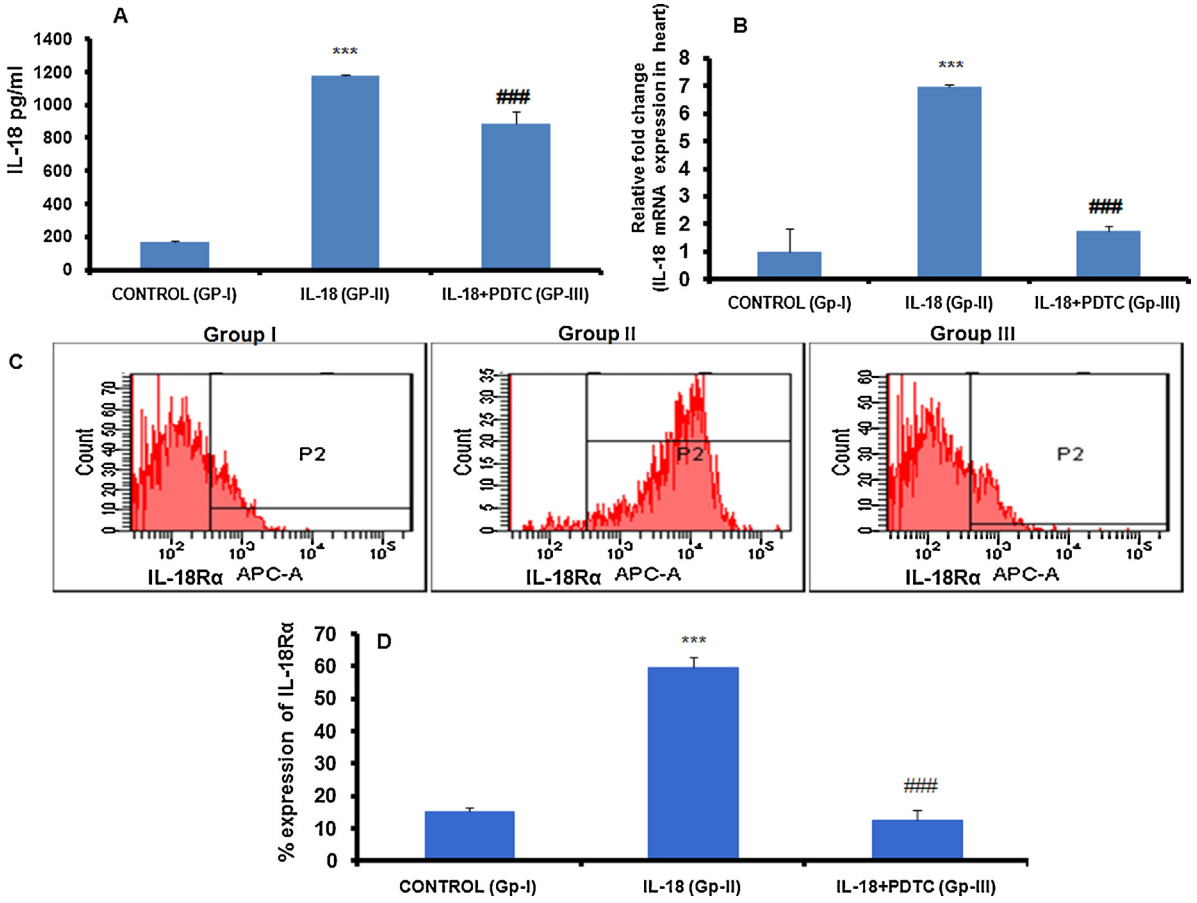

Fig. 1. Plasma IL-18 levels, IL-18 mRNA, and IL-18 Rα expression in Apo E−/− mice. (A) Representative bar diagram showing circulatory levels of IL-18 (pg/ml). (B) mRNA expression of IL-18. (C) Histogram represents the fluorescence intensity of IL-18 Rα antibody. (D) Bar graph represents % expression of IL-18 Rα. IL-18 Rα [allophycocyanin (APC)-conjugated rat monoclonal anti-mouse IL-18 Rα], Gp I (phosphate-buffered saline injected for 2 months), Gp II (recombinant IL-18 for 1 month followed by phosphate-buffered saline for 1 month), and Gp III (recombinant IL-18 for 1 month followed by PDTC for 1 month) ($n = 6$) ($^{***}p < 0.001$ vs. Gp I, $^{###}p < 0.001$ vs. Gp II). IL, interleukin; R, receptor; Apo, apolipoprotein; PDTC, pyrrolidine dithiocarbamate.

(24.03 ± 3.35 vs. 25.07 ± 2.06 g, 25.91 ± 3.9 g), respectively. A significant increase in serum TC and LDL-C and a significant decrease in HDL-C levels were observed in Group II mice vs. Group I (Fig. 2A). However, a significant decrease in serum TC and LDL-C, and a significant increase in HDL-C levels was observed in Group III mice vs. Group II (Fig. 2A). The change in TG and VLDL-C levels was statistically non-significant.

Expression of CD36 and MMP-9 in IL-18-treated Apo E−/− mice

We observed significantly augmented, i.e. ~8-fold and ~3-fold mRNA expression of the CD36 and MMP-9 in heart and aortic tissues of Group II mice ($p < 0.001$; Figs. 2B and 3A), whereas these were significantly downregulated ~7-fold and ~2.8-fold in Group III animals. We also examined protein expression of CD36 in heart (Fig. 2C) and MMP-9 expression in aorta by immunohistochemistry (Fig. 3B). An increased CD36 expression was observed in cardiomyocytes and microvascular endothelial cells, whereas MMP-9 expression was increased in the endothelial cell lining in Group II mice vs. Group I, and a reduced expression was noted in Group III animals.

Transcriptional/translation expression of LXR-α in IL-18-treated Apo E−/− mice

We examined LXR-α mRNA expression in pooled heart tissues. LXR-α mRNA expression was found to be significantly attenuated in Group II mice vs. Group I ($p < 0.001$). However, LXR-α expression was significantly increased in Group III animals (Fig. 3A). Similar results were observed by immunohistochemistry analysis where Group II mice had reduced LXR-α protein expression in cardiomyocytes as compared to Group I, and its expression was augmented in Group III mice (Fig. 3B).

Transcriptional/translation expression of NF-κB p65 RelA in IL-18-treated Apo E−/− mice

A significantly augmented mRNA expression of NF-κB was observed in heart tissues of Group II mice, i.e. ~7-fold vs. Group I ($p < 0.001$; Fig. 3A) and it was significantly downregulated in Group III animals. Further, we also examined expression of NF-κB p65 protein in heart sections by immunohistochemistry. An augmented NF-κB p65 expression was observed in cardiomyocytes of Group II animals as compared to the Group I and Group III animals (Fig. 3B).

Histological examination, Masson's trichrome and ORO staining

Based on hematoxylin and eosin stains, we observed increased percentage of atheromatous lesions in aorta of Group II vs. Group I and Group III mice. No remarkable changes were observed in any of the groups in heart and coronary arteries (Fig. 4A–C). MT staining demonstrated different grades of atherosclerotic lesions in aorta. Increased number of foam cells, inflammatory cells, smooth muscle cells and collagen were present in the lesions of Group II mice (Fig. 5A). Based on ORO staining, a significant increase in percentage lesion area in the ascending aorta and aortic arch was observed in Group II mice vs. Group I (24.09 ± 13.32% vs. 1.52 ± 0.57%; $p < 0.001$) whereas a significant decrease was observed in PDTC-treated Group III animals (24.09 ± 13.32% vs. 3.37 ± 0.99%; $p < 0.001$; Gp II vs. Gp III; Fig. 5B and C).

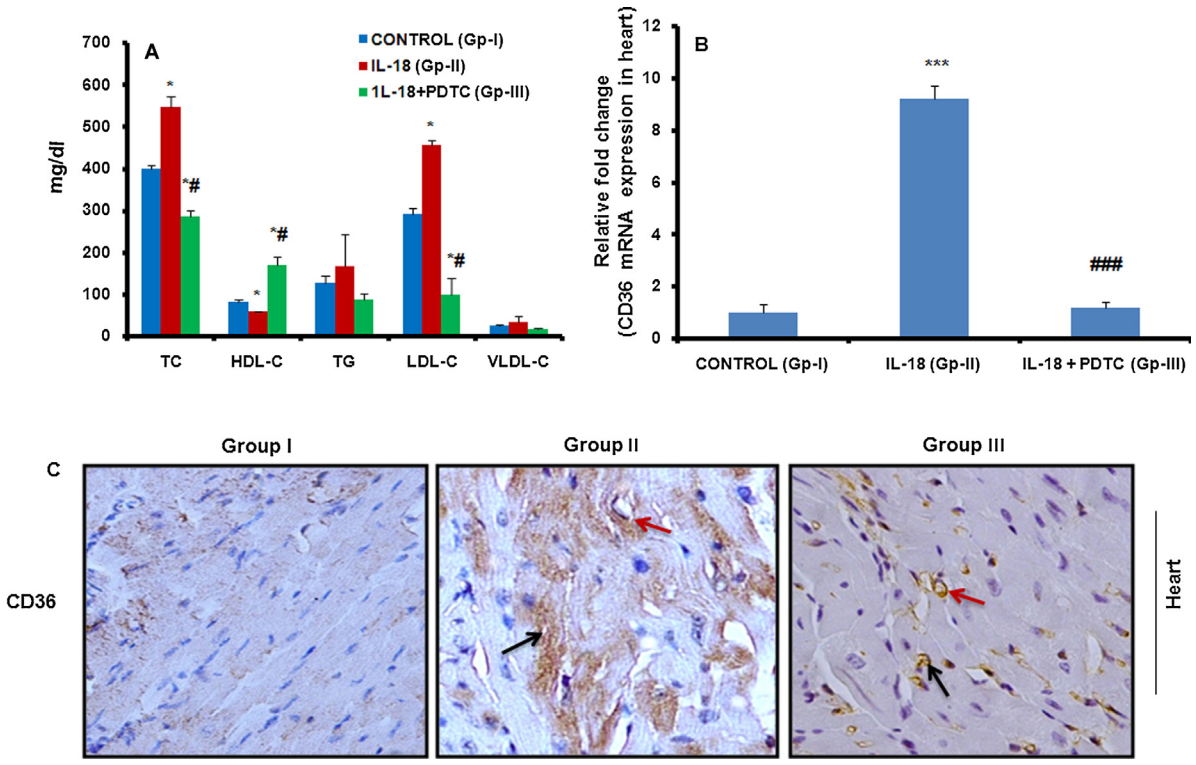

Fig. 2. Lipid and lipoprotein profile and scavenger receptor CD36 expression in apolipoprotein E−/− mice. (A) Representative bar diagram shows lipid and lipoprotein profile (mg/dl). (B) mRNA expression of CD36. (C) Sections from heart showing CD36 immunostaining rabbit polyclonal anti-mouse. CD36 is indicated by black arrow (brown stain) in cardiomyocytes and microvascular endothelial cells by red arrow. Original magnifications, C, ×400. Gp I (phosphate-buffered saline injected for 2 months), Gp II (recombinant IL-18 for 1 month followed by phosphate-buffered saline for 1 month), Gp III (rIL-18 for 1 month followed by PDTC for 1 month) ($n = 6$) ($^{*}p < 0.05$ vs. Gp I; $^{\#}p < 0.05$ vs. Gp II; $^{***}p < 0.001$ vs. Gp I, $^{\#\#\#}p < 0.001$ vs. Gp II). TC, total cholesterol; HDL-C, high-density lipoprotein cholesterol; TG, triglycerides; LDL-C, low-density lipoprotein cholesterol; VLDL-C, very low-density lipoprotein cholesterol; IL, interleukin. (For interpretation of the references to color in this figure legend, the reader is referred to the web version of this article.)

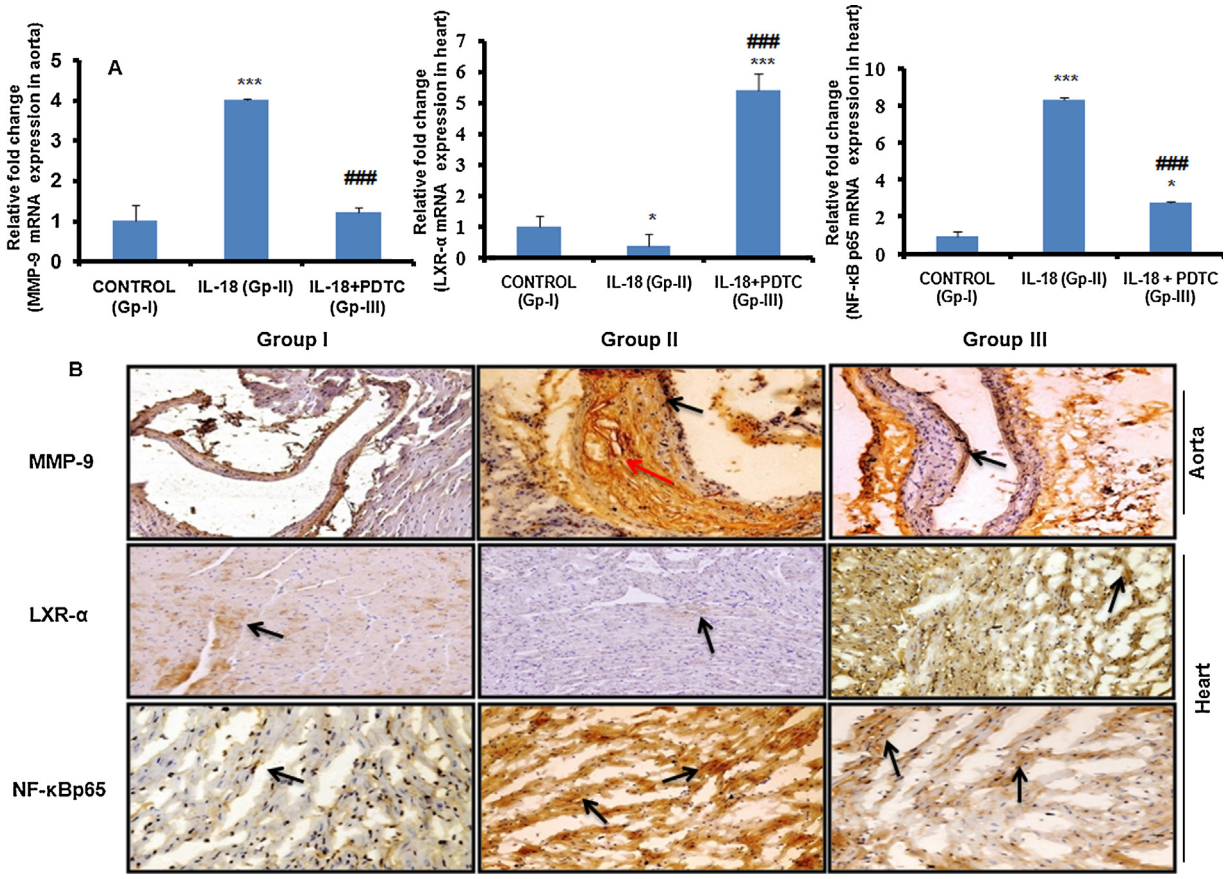

Fig. 3. mRNA expression and immunohistochemical analysis of MMP-9, LXR-α, and NF-κB p65 in apolipoprotein E−/− mice. (A) mRNA expression of MMP-9, LXR-α and NF-κB p65. (B) Representative sections from heart and aorta [atherosclerotic plaques (red arrow)]. MMP-9 immunostaining goat polyclonal anti-mouse MMP-9 in aorta is indicated by black arrow (brown stain) in endothelial cell lining, LXR-α immunostaining goat polyclonal anti-mouse LXR-α in heart sections is indicated by black arrow (brown stain) in cardiomyocytes, and NF-κB p65 immunostaining rabbit polyclonal anti-mouse NF-κB p65 in heart sections is indicated by black arrow (brown stain) in cardiomyocytes. Gp I (phosphate-buffered saline injected for 2 months), Gp II (recombinant IL-18 for 1 month followed by phosphate-buffered saline for 1 month), Gp III (recombinant IL-18 for 1 month followed by PDTC for 1 month) ($n = 6$). Original magnifications, ×200 ($^{*}p < 0.05$ vs. Gp I; $^{***}p < 0.001$ vs. Gp I, $^{\#\#\#}p < 0.001$ vs. Gp II). MMP-9, matrix metalloproteinase-9; LXR-α, Liver X receptor alpha; NF-κB, nuclear factor kappa-B; IL, interleukin; PDTC, pyrrolidine dithiocarbamate. (For interpretation of the references to color in this figure legend, the reader is referred to the web version of this article.)

Discussion

Our results clearly indicate a crucial role of pro-inflammatory cytokine IL-18 in atherosclerotic plaque development, progression, and stability. Only two studies reported in mice models have reported that IL-18 administration promotes development of atherosclerosis [11,16]. Mallat et al. demonstrated increased IL-18 expression in human carotid atherosclerotic plaques [7]. In the current study, administration of rIL-18 in Apo E−/− mice initiated an inflammatory response that was associated with upregulation of cell adhesion molecules like ICAM-1 and VCAM-1 (data not shown) resulting in endothelial dysfunction. Endothelial dysfunction and presence of increased oxidative stress may give rise to increased Ox-LDL levels. Although we did not determine Ox-LDL levels, a significantly increased scavenger receptor (CD36) expression with IL-18 administration in our study could be due to raised Ox-LDL that may lead to foam cell formation and thus development and progression of atherosclerosis. CD36 mRNA expression has been shown to be upregulated in macrophages by inflammatory cytokines, and blocking CD36 expression or its downstream signaling is shown to inhibit Ox-LDL uptake and limit experimental atherosclerosis in mice [17,18]. Another mechanism of lipid-independent atherosclerotic plaque development due to IL-18 could be due to increased MMP-9 expression in the present study. IL-18 has been shown to induce MMPs in murine peritoneal macrophages and human monocytes [19,20]. Our data demonstrated that atherosclerotic plaques were rich in inflammatory cells, smooth muscle cells, and collagen, thus induction of MMP-9 via IL-18 may be a crucial link in the chain of events promoting plaque rupture, thrombosis, and myocardial infarction. Further, interferon (IFN)-γ and IL-6 induction by IL-18 could be another mechanism by which IL-18 may increase atherosclerosis independent of cholesterol levels. In this context, in IL18 −/− × Apo E−/− mice, reduced lesion size and lesion composition was observed which was found to be independent of cholesterol and triglycerides and lack of IFN-γ release [21].

Significantly augmented plasma IL-18 levels and IL-18 mRNA expression in our study also support the above statement. Increased serum IL-18 levels were found to be positively correlated with carotid intima media thickness (IMT) and coronary atherosclerosis in type II diabetics and myocardial infarction patients, respectively [22,23]. Our data are in tune with these reports and are also strengthened by finding increased IL-18 Rα expression on PBMCs with rIL-18 treatment in our study.

A significant downregulation of IL-18-induced molecules such as IL-18, IL-18 Rα, CD36, MMP-9, NF-κB, and upregulation of LXR-α was observed with PDTC demonstrating that IL-18 acts through NF-κB pathway. PDTC is well tolerated below 50 mg/kg in vivo [12]. In RA synovial fibroblasts, PDTC has been shown to inhibit IL-18-induced NF-κB activation and IL-18 has been shown to activate

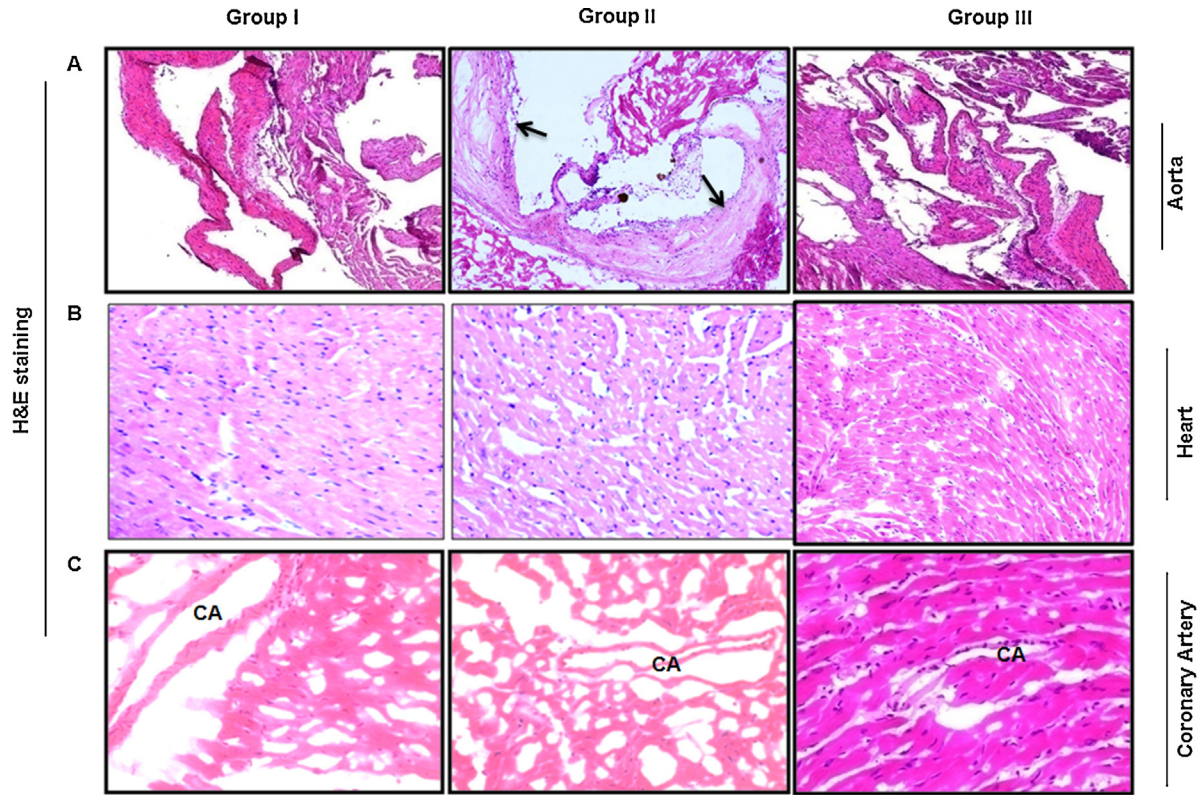

Fig. 4. Hematoxylin and eosin (H&E) staining of heart, aorta, and coronary artery (CA) of apoliprotein E−/− mice. Representative sections from heart, aorta, and CA showing atherosclerotic plaques (arrow) and CA (H&E stain). Gp I (phosphate-buffered saline injected for 2 months), Gp II (recombinant interleukin-18 for 1 month followed by phosphate-buffered saline for 1 month), and Gp III (recombinant interleukin-18 for 1 month followed by pyrrolidine dithiocarbamate for 1 month) ($n = 6$). Original magnifications, A ×100, B ×200 and C ×400.

both NF-κB and AP-1 in vascular smooth muscle cells (VSMCs) [24,25]. IL-18 binding to IL-18 Rα results in upregulation of IL-1R-associated kinase (IRAK) and tumor necrosis factor (TNF) receptor-associated factor 6 (TRAF-6) resulting in nuclear translocation of NF-κB in mouse cell lines [26]. Bond et al. [27] reported that NF-κB activity was required for upregulation and production of MMP-9 in rabbit and human VSMCs. Both MMP-2 and MMP-9 were found to be significantly decreased with PDTC treatment in spontaneously hypertensive rats [28]. These studies support our findings that inhibition of NF-κB downregulates IL-18-induced proinflammatory genes.

Various studies using LXR knockouts and LXR agonists suggest that LXR-α is not only an important regulator of cholesterol efflux in macrophages [29]. It is also anti-inflammatory and antagonizes the process of Ox-LDL uptake and foam cell formation, thus preventing atherosclerotic lesion formation. *Our observation that IL-18 attenuates LXR-α in a* NF-κB *dependent manner is the first report in the literature*.

Our findings demonstrate that IL-18 administration increased serum cholesterol and lipoprotein-cholesterol distribution in mice. Contrary to our reports, few studies did not demonstrate any effects of IL-18 on cholesterol levels [11,16]. Apo E−/− mice are known to accumulate cholesterol-rich remnant particles with plasma cholesterol levels reaching 400 mg/dl, even when fed a regular low-fat, low-cholesterol diet. Also, humans lacking apo E (extremely rare) are reported to have elevated remnant cholesterol in plasma [30].

Chronic systemic inflammation through IL-18 may give rise to dysfunctional or proinflammatory HDL and therefore may cause dysregulated reverse cholesterol transport, thus resulting in increased cholesterol levels due to IL-18. Cholesterol levels can increase due to isoprenoid generation by endogenous cellular cholesterol synthesis as well as by cholesterol synthesis in activated monocytes during the inflammatory response. Isoprenoids are an integral component of the signaling pathway for IL-6-mediated inflammation and there is plenty of evidence in the literature demonstrating that IL-18 induces IL-6 production both in vitro and in vivo [31,32]. Increased IL-6 production may give rise to increased C-reactive protein (CRP) levels which could also be a trigger for increased cholesterol levels as statin-like drugs are shown to lower LDL-C and non-HDL-C and thus also lower levels of CRP.

Our data demonstrated significant atherosclerotic lesion development post-IL-18 treatment, highlighting its role as a proatherogenic cytokine. Also, a robust hypolipidemic effect of PDTC was observed in our study as compared to the controls. PDTC has been shown to attenuate plasma TG and VLDL-C and restore HDL-C levels in obese db/db mice via reduction in TNF-α and IL-6 levels [33].

Although a partial inhibition of IL-18 levels was observed in Group III mice, it almost abolished the atherosclerotic lesions in this group. These findings may be explained on the basis of the involvement of upstream and downstream players in IL-18 signaling leading to atherosclerotic changes. Significant neutralization of IL-18-induced signaling by PDTC as observed via blockage of IL-18 as well as NF-κB activation could be responsible for the observed effect. Our findings are further strengthened by a report which observed that inhibiting NF-κB activity reduces atherosclerosis in Apo E/LDLR^{-} double knockout (KO) mice [34].

To the best of our knowledge, our study is the first report in the literature that demonstrates that exogenous rIL-18 administration significantly upregulates CD36 and MMP-9 expression via NF-κB pathway, thus suggesting a crosstalk involved in the progression and destabilization of atherosclerotic plaques. Downregulation of

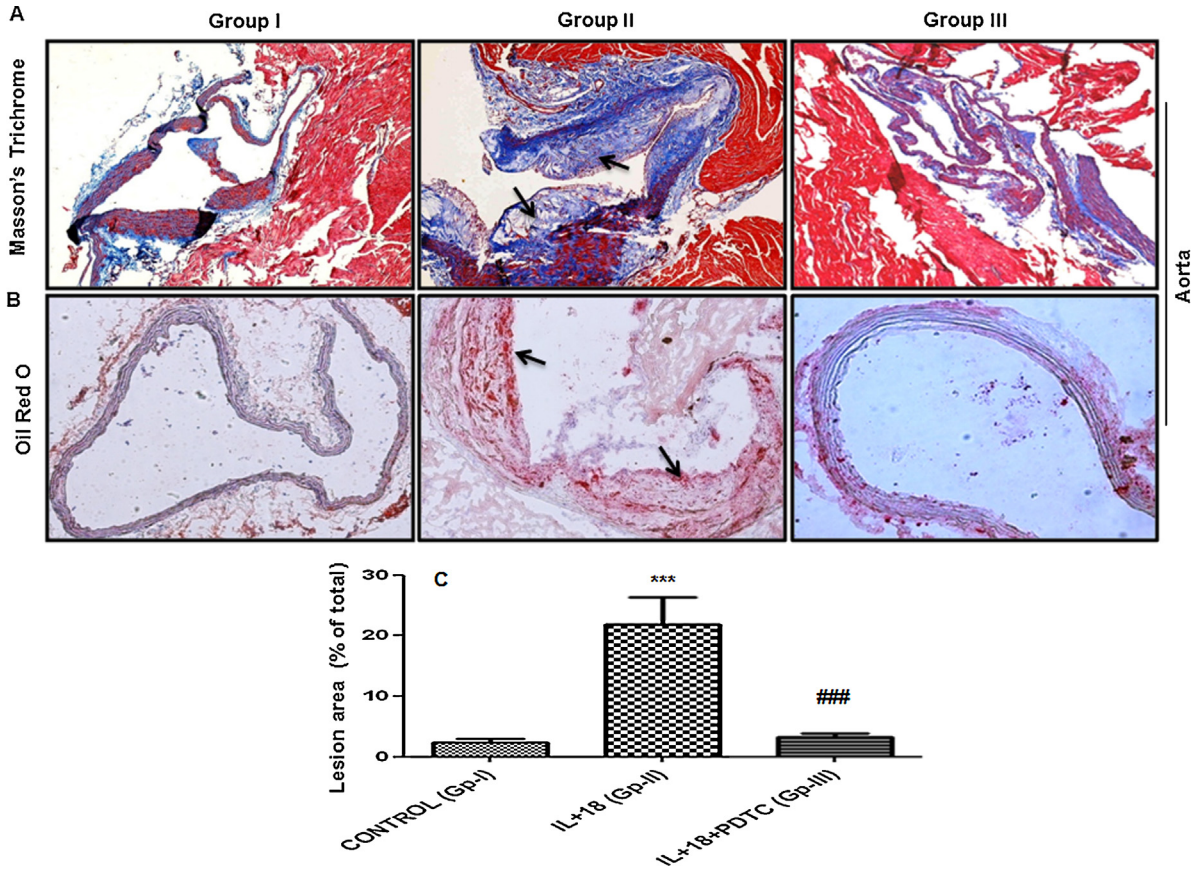

Fig. 5. Characterization and quantification of atherosclerotic lesions in apolipoprotein E−/−mice. (A) Masson's trichrome staining in sections of aorta. Collagen deposition (blue; arrow) and muscle fibers (red). (B) Oil Red O staining in sections of aorta showing lipid deposition (atherosclerotic plaques) (arrow). (C) Bar graph represents quantitative computer-assisted image analysis of lipid deposition. Gp I (phosphate-buffered saline injected for 2 months), Gp II (recombinant IL-18 for 1 month followed by phosphate-buffered saline for 1 month), and Gp III (rIL-18 for 1 month followed by PDTC for 1 month) ($n = 6$). Original magnifications, A ×100 and B ×200 ($^{***}p < 0.001$ vs. Gp I, $^{###}p < 0.001$ vs. Gp II). IL, interleukin; PDTC, pyrrolidine dithiocarbamate. (For interpretation of the references to color in this figure legend, the reader is referred to the web version of this article.)

LXR-α by IL-18 and its upregulation by PDTC is another significant observation in our study. Our data also shows that PDTC protects against IL-18-induced atherosclerosis via NF-κB inhibition.

Concluding, our study highlights IL-18 and NF-κB as important therapeutic targets for prevention of atherosclerotic plaque development and to limit plaque complications. These findings open up a new vista for future research in human subjects to explore the molecular targets of IL-18 and NF-κB-mediated signaling.

Source of funding

We thank Department of Biotechnology, New Delhi, India, for providing the financial support.

Conflict of interest/disclosure

None.

Acknowledgements

We thank Dr B Sesikeran, Director, National Institute of Nutrition (NIN), Hyderabad for providing facilities at the Institute.

References

[1] Libby P, Ridker PM, Maseri A. Inflammation and atherosclerosis. Circulation 2002;105:1135–43.
[2] Repa JJ, Mangelsdorf DJ. The liver X receptor gene team: potential new players in atherosclerosis. Nat Med 2002;8:1243–8.
[3] Berliner JA, Navab M, Fogelman AM, Frank JS, Demer LL, Edwards PA, Watson AD, Lusis AJ. Atherosclerosis: basic mechanisms: oxidation, inflammation and genetics. Circulation 1995;91:2488–96.
[4] Raffetto JD, Khalil RA. Matrix metalloproteinases and their inhibitors in vascular remodeling and vascular disease. Biochem Pharmacol 2008;75:346–59.
[5] Zhang SH, Reddick RL, Piedrahita JA, Maeda N. Spontaneous hypercholesterolemia and arterial lesions in mice lacking apolipoprotein E. Science 1992;258:468–71.
[6] Nakashima Y, Plump AS, Raines EW, Breslow JL, Ross R. ApoE-deficient mice develop lesions of all phases of atherosclerosis throughout the arterial tree. Arterioscler Thromb 1994;14:133–40.
[7] Mallat Z, Corbaz A, Scoazec A, Besnard S, Leseche G, Chvatchko Y, Tedgui A. Expression of interleukin-18 in human atherosclerotic plaques and relation to plaque instability. Circulation 2001;104:1598–603.
[8] Mallat Z, Corbaz A, Scoazec A, Graber P, Alouani S, Esposito B, Humbert Y, Chvatchko Y, Tedgui A. Interleukin-18/interleukin-18 binding protein signaling modulates atherosclerotic lesion development and stability. Circ Res 2001;89:e41–5.
[9] Hoshino K, Tsutsui H, Kawai T, Takeda K, Nakanishi K, Takeda Y, Akira S. Cutting edge: generation of IL-18 receptor-deficient mice: evidence for IL-1 receptor-related protein as an essential IL-18 binding receptor. J Immunol 1999;162:5041–4.
[10] Piedrahita JA, Zhang SH, Hagaman JR, Oliver PM, Maeda N. Generation of mice carrying a mutant apolipoprotein-E gene inactivated by gene targeting in embryonic stem cells. Proc Natl Acad Sci USA 1992;89:4471–5.
[11] Whitman SC, Ravisankar P, Daugherty A. Interleukin-18 enhances atherosclerosis in apolipoprotein E(−/−) mice through release of interferon-gamma. Circ Res 2002;90:E34–8.
[12] Cuzzocrea S, Chatterjee PK, Mazzon E, Dugo L, Serraino I, Britti D, Mazzullo G, Caputi AP, Thiemermann C. Pyrrolidine dithiocarbamate attenuates the development of acute and chronic inflammation. Br J Pharmacol 2002;135:496–510.
[13] Whitman SC, Ravisankar P, Elam H, Daugherty A. Exogenous interferon-γ enhances atherosclerosis in apolipoprotein E−/− mice. Am J Pathol 2000;157:1819–24.

[14] Friedwald WT, Levy RI, Fredrickson DS. Estimation of the concentration of low-density lipoprotein cholesterol in plasma without use of the preparative ultracentrifuge. Clin Chem 1972;18:499–502.
[15] Livak KJ, Schmittgen TD. Analysis of relative gene expression data using Real-Time Quantitative PCR and the 2 (−Delta Delta C (T)) Method. Methods 2001;25:402–8.
[16] Tenger C, Sundborger A, Jawien J, Zhou X. IL-18 accelerates atherosclerosis accompanied by elevation of IFN-γ and CXCL16 expression independently of T cells. Arterioscler Thromb Vasc Biol 2005;25:791–6.
[17] Silverstein RL. Inflammation, atherosclerosis, and arterial thrombosis: role of the scavenger receptor CD36. Cleve Clin J Med 2009;76:S27–30.
[18] Guy E, Kuchibhotla S, Silverstein R, Febbraio M. Continued inhibition of atherosclerotic lesion development in long term Western diet fed CD36o/Apo Eo mice. Atherosclerosis 2007;192:123–30.
[19] Gerdes N, Sukhova GK, Libby P, Reynolds RS, Young JI, Schonbeck U. Expression of IL-18 and functional IL-18 receptor on vascular endothelial cells, smooth muscle cells and macrophages: implications for atherogenesis. J Exp Med 2002;195:245–57.
[20] Quiding-Jarbank M, Smith DA, Bancroft GJ. Production of matrix metalloproteinases in response to mycobacterial infection. Infect Immun 2001;69:5661–70.
[21] Elhage R, Jawien J, Rudling M, Ljunggren HG, Takeda K, Akira S, Bayard F, Hansson GK. Reduced atherosclerosis in interleukin-18 deficient apolipoprotein E-knockout mice. Cardiovasc Res 2003;59:234–40.
[22] Nakamura A, Shikata K, Hiramatsu M, Nakatou T, Kitamura T, Wada J, Itoshima T, Makino H. Serum interleukin-18 levels are associated with nephropathy and atherosclerosis in Japanese patients with type 2 diabetes. Diabetes Care 2005;28:2890–5.
[23] Hulthe J, McPheat W, Samnegard A, Tornvall P, Hamsten A, Eriksson P. Plasma interleukin-18 concentration is elevated in patients with previous myocardial infarction and related to severity of coronary atherosclerosis independently of C-reactive protein and IL-6. Atherosclerosis 2006;188:450–4.
[24] Morel JC, Park CC, Woods JM, Koch AE. A novel role for interleukin-18 in adhesion molecule induction through NF kappa B and phosphatidyl-inositol (PI) 3-kinase dependent signal transduction pathways. J Biol Chem 2001;276:37069–75.
[25] Sahar S, Dwarakanath RS, Reddy MA, Lanting L, Todorov I, Natarajan R. Angiotensin II enhances interleukin-18 mediated inflammatory gene expression in vascular smooth muscle cells. A novel cross-talk in the pathogenesis of atherosclerosis. Circ Res 2005;96:1064–71.
[26] Matsumoto S, Tsuji-Takayama K, Aizawa Y, Koide K, Takeuchi M, Ohta T, Kurimoto M. Interleukin-18 activates NF-KB in murine T helper type 1 cells. Biochem Biophys Res Commun 1997;234:454–7.
[27] Bond M, Chase AJ, Baker AH, Newby AC. Inhibition of transcription factor NF-κB reduces matrix metalloproteinase-1, -3 and -9 production by vascular smooth muscle cells. Cardiovasc Res 2001;50:556–65.
[28] Wu KI, Schmid-Schönbein GW. Nuclear factor kappa B and matrix metalloproteinase induced receptor cleavage in the spontaneously hypertensive rat. Hypertension 2011;57:261–8.
[29] Venkateswaran A, Laffitte BA, Joseph SB, Mak PA, Wilpitz DC, Edwards PA, Tontonoz P. Control of cellular cholesterol efflux by the nuclear oxysterol receptor LXR alpha. Proc Natl Acad Sci USA 2000;97:12097–102.
[30] Schaefer EJ, Gregg RE, Ghiselli G, Forte TM, Ordovas JM, Zech LA, Brewer HB. Familial apolipoprotein E deficiency. J Clin Invest 1986;78:1206–19.
[31] Netea MG, Kullberg BJ, Verschueren I, Van Der Meer JW. Interleukin-18 induces production of proinflammatory cytokines in mice: no intermediate role for the cytokines of the tumor necrosis factor family and interleukin-1beta. Eur J Immunol 2000;30:3057–60.
[32] Jablonska E, Jablonski J. Effect of IL-18 on the release of IL-6 and its soluble receptors: sIL-6Ralpha and sgp130 by human neutrophils. Immunol Invest 2002;31:159–67.
[33] Mariappan N, Elks CM, Sriramula S, Guggilam A, Liu Z, Borkhsenious O, Francis J. NF-κB-induced oxidative stress contributes to mitochondrial and cardiac dysfunction in type II diabetes. Cardiovasc Res 2010;85:473–83.
[34] Jawień J, Gajda M, Mateuszuk Ł, Olszanecki R, Jakubowski A, Szlachcic A, Korabiowska M, Korbut R. Inhibition of nuclear factor-κB attenuates atherosclerosis in Apo E/LDLR – double knockout mice. J Physiol Pharmacol 2005;56:483–9.